Original Article
Activation of the CXCL16/CXCR6 pathway promotes lipid deposition in fatty livers of apolipoprotein E knockout mice and HepG2 cells

Kun Ling Ma[1], Yu Wu[1], Yang Zhang[1], Gui Hua Wang[1], Ze Bo Hu[1], Xiong Zhong Ruan[2]

[1]Institute of Nephrology, Zhong Da Hospital, School of Medicine, Southeast University, Nanjing, Jiangsu Province, China; [2]Centre for Nephrology, University College London (UCL) Medical School, Royal Free Campus, UK

Abstract: Non-alcoholic fatty liver disease (NAFLD), characterised by early lipid accumulation and subsequent inflammation in the liver, is becoming a worldwide challenge due to its increasing prevalence in developing and developed countries. This study aimed to investigate the role of CXC chemokine ligand 16 (CXCL16) and its receptor CXC chemokine receptor 6 (CXCR6) in NAFLD under inflammation. We used IL-1β stimulation in human hepatoblastoma cell line (HepG2) for *in vitro* studies and casein injection in apolipoprotein E knockout mice *in vivo* to induce inflammatory stress. The effects of inflammation on cholesterol accumulation were examined by histochemical staining and a quantitative intracellular cholesterol assay. The gene and protein expression of molecules involved in CXCL16/CXCR6 pathway and extracellular matrix (ECM) were examined by real-time polymerase chain reaction (PCR) and Western blotting. The fluorescence intensity of reactive oxygen species (ROS) was assessed by flow cytometry. Results showed that significantly elevated levels of serum amyloid protein A in casein-injected mice confirmed the successful induction of inflamed NAFLD model. Inflammation significantly increased lipid accumulation in livers compared with the high-fat diet group and the controls. Furthermore, inflammation increased the expression of CXCL16, CXCR6, and adisintegrin and metalloproteinase domain-containing protein 10 (ADAM10) in livers, accompanied with increased ECM expression and ROS production. These effects were further confirmed by *in vitro* studies. Interestingly, CXCL16 gene knockdown in HepG2 cells induced by CXCL16 siRNA resulted in decreased lipid accumulation, ECM excretion, and ROS production. These findings demonstrated that inflammation-mediated activation of CXCL16/CXCR6 is involved in the progression of NAFLD.

Keywords: Non-alcoholic fatty liver disease, inflammatory stress, CXCL16/CXCR6 pathway

Introduction

Non-alcoholic fatty liver disease (NAFLD) is increasingly recognised as a leading cause of liver dysfunction and cirrhosis in the developed world and is a part of the spectrum of metabolic diseases associated with obesity, dyslipidemia, insulin resistance, and type 2 diabetes mellitus [1, 2]. NAFLD presents as a spectrum of pathologies ranging from benign steatosis defined by accumulation of triglycerides and other glycerophospolipids in hepatocytes and progresses to non-alcoholic steatohepatitis (NASH) characterised by the development of concomitant inflammation in the liver [3]. NASH is a unique liver microenvironment marked by accumulation of triglycerides, characteristic pathologic findings such as Mallory bodies and

the infiltration of inflammatory cells [4]. As time goes on, NASH progresses to end-stage liver disease with fibrosis and cirrhosis, and even hepatocellular cancer. Conventional models include a "two-hit" and "multi-hit" hypothesis of NAFLD in which the dysregulated lipid metabolism and insulin resistance are considered the "first hit" and the following "second hit" or "multi-hit" likely involve oxidative stress, lipid peroxidation, and subsequent inflammatory responses [5]. However, the exact mechanisms of inflammatory stress in the progression of NAFLD have not been completely elucidated.

Liver inflammation in general is tightly controlled by chemokines, which are peptide mediators that stimulate the chemotaxis of target cells through specific G protein-coupled recep-

tors [6]. Recently, a novel chemokine, CXC chemokine ligand 16 (CXCL16) was found, which was found to be widely expressed in immune cells, smooth muscle cells, and endothelial cells [7]. Matloubian [8] and Wilbanks [9] demonstrated that CXCL16 exists in a transmembrane-bound and soluble form. Transmembrane-bound CXCL16 has two functions [10]: as a cell surface adhesion molecule, it might mediate T-cell adhesion to the endothelium; as a novel scavenger receptor, it mediates the uptake of atherogenic lipoproteins by macrophages and smooth muscle cells [11]. Furthermore, transmembrane-bound CXCL16 can be released to its soluble form upon digestion by adisintegrin and metalloproteinase domain-containing protein 10 (ADAM10) [12]. Soluble CXCL16 can recruit activated immune cells expressing CXC chemokine receptor 6 (CXCR6), the receptor of CXCL16, including CD8+T cells, CD4+T cells, natural killer (NK) cells, invariant natural killer T (NKT) cells, plasma cells and monocytes. Soluble CXCL16 enhances transendothelial mesenchymal stem cell migration [13] and facilitates immune cell migration to sites of inflammation, such as inflamed liver [14].

Recently, several lines of evidence have shown that activation of CXCL16 is involved in the progression of kidney diseases. Serum CXCL16 levels were higher in patients with lupus nephritis [15], diabetic nephropathy and nephritic syndrome [16] when compared with healthy people. In addition, CXCL16 and its receptor CXCR6 play crucial roles in the pathogenesis of atherosclerosis by mediating oxidative low-density lipoprotein (oxLDL) engulfment by macrophages and smooth muscle cells, which then develop into cholesterol-filled foam cells. CXCL16 acts as chemoattractants, activating and attracting CD8+T cells to sites of inflammation [11]. Moreover, Wehr et al. [17] showed that hepatic NKT cells become CXCR6-dependent early upon injury, thereby accentuating the inflammatory response in the liver and promoting hepatic fibrogenesis. Interfering with CXCL16/CXCR6 might, therefore, have therapeutic potential in liver fibrosis.

Although plenty of studies have demonstrated the role of the CXCL16/CXCR6 pathway in kidney diseases, atherosclerosis, and liver injuries, little is known about its function in the progression of NAFLD, especially under subsequent inflammation during the second hit phase. Our previous study demonstrated that increased mammalian target of rapamycin complex 1 (mTORC1) activity mediated by inflammation exacerbates the progression of NAFLD by disrupting low-density lipoprotein receptor expression at the transcriptional and posttranscriptional levels [18]. Therefore, this study aimed to investigate the role of the CXCL16/CXCR6 pathway in NAFLD under the condition of inflammation in vivo and in vitro.

Materials and methods

Animals

Male apolipoprotein E knockout (ApoE KO) mice were kindly provided by Animal Care of Chong Qing Medical University. The mice were maintained under a constant 12-hour photoperiod at temperatures between 21°C and 23°C and were allowed free access to food and water. Eight-week-old ApoE KO mice were randomly assigned and fed with a normal diet containing 4% fat (control group, n=8), or a high-fat diet containing 21% fat and 0.15% cholesterol (HF group, n=8), or a high-fat diet plus daily 0.5 ml 10% casein (100 grams of casein dissolved in 1 litre of water with 4.2 grams of sodium bicarbonate) subcutaneous injection (HF+casein group, n=8) for 8 weeks. When the experiments were terminated at the 8th week, the blood was sampled from right heart ventricle for biochemical assays. Isolated liver samples were used for histological assessments. The protocols used in experiments were approved by the Committee on the Ethics of Animal Experiments of Southeast University. The methods were carried out in accordance with the approved guidelines. All surgeries were performed under sodium pentobarbital anesthesia to minimize suffering.

Enzyme-linked immunosorbent assay

The serum amyloid protein A (SAA) was measured using commercial kits (Invitrogen, USA).

Plasma lipid profile analysis

Using blood samples obtained from the mice at termination, Serum concentrations of triglyceride (TG), total cholesterol (TC), high-density lipoprotein (HDL) and LDL were determined by automatic analysers (Hitachi, Japan).

Haematoxylin-eosin (HE) staining

Livers tissues embedded in paraffin were sectioned and dewaxed. Sections were then stained for 15 minutes with haematoxylin, subsequently stained for 3 minutes by 1% eosin. After dehydration, resinene was used to seal the sections to transparency. The sections were observed under light microscopy (×400).

Filipin staining

Samples were fixed with 5% paraformaldehyde for 30 minutes, washed with phosphate buffered saline (PBS), and incubated with freshly prepared Filipin solution for 30 minutes. The slides were then washed with PBS, a drop of phenylenediamine/glycerol was added, and the slides were mounted with cover slips and examined by laser confocal microscopy (×200).

Immunohistochemical staining

The sections embedded in paraffin were previously deparaffinised and treated with 0.3% endogenous peroxidase blocking solution for 15 minutes. Sections were then treated sequentially with normal nonimmune animal serum for 30 minutes and incubated with anti-mouse polyclonal primary antibodies targeting CD68 (Novus Biologicals Inc., Canada), monocyte chemotactic protein 1 (MCP-1, Santa Cruz Biotechnology Inc., USA), tumour necrosis factor-α (TNF-α, Santa Cruz Biotechnology Inc., USA), CXCL16 (R&D Systems Inc., USA), CXCR6 (Novus Biologicals Inc., Canada), ADAM10 (Abcam, UK), collagen I (Abcam, UK) and α-smooth muscle actin (α-SMA, Abcam, UK) at 4°C overnight. Sections were then incubated with biotin-labelled secondary antibodies (Maixin Biotechnology Ltd., China) for 30 minutes at room temperature, followed by incubation with streptomycete antibiotin-peroxidase for another 10 minutes. Staining was completed by a 3-minute incubation with 3, 3'-diaminobenzidine substrate-chromogen, which resulted in a brown-coloured precipitate at the antigen site. Counterstaining was performed with haematoxylin. Immunohistochemical images were acquired by light microscope (×400).

Cell culture

An established human hepatoblastoma cell line (HepG2, Tumour Cell Bank of the Chinese Academy of Sciences, China) was used in all experiments. The cells were cultured with Dulbecco's Modified Eagle's Medium (DMEM) containing 10% fetal bovine serum (Gibco, USA). The cells were incubated with the condition of 5% CO_2 at 37°C. At 70%-80% confluence, the cells were synchronised with a serum-free culture medium for 24 hours and subsequently stimulated with 30 μg/ml cholesterol (Sigma, USA) or with 5 ng/ml interleukin-1β (IL-1β, R&D systems Inc., USA) for another 24 hours.

Quantitative measurements of intracellular free cholesterol/cholesterol ester

Quantitative measurements of intracellular total and free cholesterol were measured using previous method [19]. Briefly, the lipids were extracted from collected cells by adding 1 mL of chloroform/methanol (2:1). After sonication, the lipid phase was collected from centrifuged samples and then dried in a vacuum, followed by dissolved in 2-propanol containing 10% Triton X-100. The amount of total cholesterol was calculated by checking free cholesterol converted from cholesterol ester by cholesterol ester hydrolase (Sigma, USA). The concentration of total and free cholesterol per sample was analysed using a standard curve and normalised against total cell protein. The concentration of cholesterol ester was calculated by subtracting the amount of free cholesterol from the total cholesterol.

CXCL16 siRNA transfection

HepG2 cells were cultured in six-well plates and transiently transfected with the CXCL16 siRNA or an empty vector siRNA (Cell Signaling Technology, USA) using Lipofectamine 2000 (Invitrogen, USA) in accordance with the manufacturer's protocol. Briefly, 2 μL of CXCL16 siRNA was mixed with 5 μL of Lipofectamine 2000 and applied to the cells. The transfected cells were incubated at room temperature for 15 minutes and were then seeded in a well containing 250 μL of Opti-MEM medium (Gibco Life Technologies, USA). At the indicated time points, the cells were harvested and examined by Filipin staining, immunofluorescent staining, real-time polymerase chain reaction (PCR), and Western blotting.

Confocal microscopy

HepG2 cells cultured in a glass bottom dish were washed, fixed, and permeabilised. The cells were then incubated with CXCL16 (R&D

Table 1. The primers used for real-time PCR

Genes	Primer sequences
CXCL16	5'-GACTCTATGTTGCCCAGGCTGTTAT-3'-sense
	5'-GCAGTGGCTGGTTAGTCCTATGTT-3'-antisense
CXCR6	5'-CAAGAGCCTACTGGGCATCTACAC-3'-sense
	5'-TGGCCTTAACCACTACAATGAAAC-3'-antisense
ADAM10	5'-GAACTCTGCCATTTCACTCTGTCAT-3'-sense
	5'-GCATGTTCTTCTTGAGGTATCTGTG-3'-antisense
MCP-1	5'-CAGCCAGATGCAATCAATGCC-3'-sense
	5'-TGGAATCCTGAACCCACTTCT-3'-antisense
TNF-α	5'-AGGACACCATGAGCACTGAAAGC-3'-sense
	5'-AAGGAGAAGAGGCTGAGGAACAAG-3'-antisense
Collagen I	5'-CGATGGATTCCAGTTCGAGTATG-3'-sense
	5'-TGTTCTTGCAGTGGTAGGTGATG-3'-antisense
a-SMA	5'-GACAATGGCTCTGGGCTCTGTAA-3'-sense
	5'-ATGCCATGTTCTATCGGGTACTTCA-3'-antisense
Fibronectin	5'-GAGCTGCACATGTCTTGGGAAC-3'-sense
	5'-GGAGCAAATGGCACCGAGATA-3'-antisense
β-actin	5'-AAAGACCTGTACGCCAACAC-3'-sense
	5'-GTCATACTCCTGCTTGCTGAT-3'-antisense

Systems Inc., USA) and ADAM10 (Abcam, UK), followed by the secondary fluorescent antibodies (donkey anti-goat Alexa Fluor 488 for CXCL16 and donkey anti-rabbit Alexa Fluor 594 for ADAM10). After washing, the cells were examined by laser confocal microscope (Olympus, Japan). The colocalisation efficiency of CXCL16 with ADAM10 was quantified using Image-Pro Plus software, version 6.0 (×400).

Reactive oxygen species (ROS) production assay

HepG2 cells grown on cover slips were treated by stimulation for 24 hours, washed with Dulbecco's PBS and incubated with media containing 50 μmol/l 5-(and-6)-chloromethyl-27-dichlorodihydrofluoroscein diacetate acetylester (CM-H2DCFDA) for 6 hours in the dark. Culture dishes were transferred to a digital microscope from Keyence (Neu-Isenburg, Germany) to document and analyse ROS generation. The average intensity of ROS fluorescence was quantitatively measured and analysed by flow cytometry.

Real-time PCR

Total RNA was extracted from the HepG2 cells and cDNA was aquired by reverse transcription (RT) using RNAiso Plus (Takara, Japan). Real-

time PCR was performed on an ABI7300 Real-time PCR System (Applied Biosystems, USA) using SYBR Green dye. The primers used for Real-time PCR are shown in **Table 1**. β-actin served as an internal reference gene. The results were analysed using Sequence Detection software, version 1.4 (Applied Biosystems, USA). The relative gene expression of each target gene was quantified against a standard curve.

Western blotting

The identical total protein extracted from the HepG2 cells was isolated by gel electrophoresis and transferred onto polyvinylidene difluoride membranes. The membranes were then blocked by blocking buffer for one hour at room temperature. The membranes were subjected to Western blotting using anti-human polyclonal antibodies against MCP-1, TNF-α, CXCL16, CXCR6, ADAM10, collagen I, and α-SMA overnight at 4°C, followed by horseradish peroxidase-labelled secondary antibodies for one hour at room temperature. β-actin was used as an internal sample loading control and was detected with a mouse monoclonal antibody (Santa Cruz, USA). Signals were detected using an advanced ECL system (GE Healthcare, UK). Relative protein expression levels were determined by normalisation against β-actin.

Statistical analysis

All the data are expressed as the means ± standard deviation (SD) and analysed using SPSS13.0 statistical software. The Student's t-test was used to analyse the statistical significance between two groups. One-way analysis of variance (ANOVA) was used to analyse the statistical significance among multiple groups. $P < 0.05$ was considered to be statistically significant.

Results

Establishment of inflamed NAFLD model

As shown in **Figure 1A**, there was a significantly increased plasma concentration of SAA in the HF+casein group compared with the control. Immunohistochemical staining and Western blotting demonstrated that there was increased
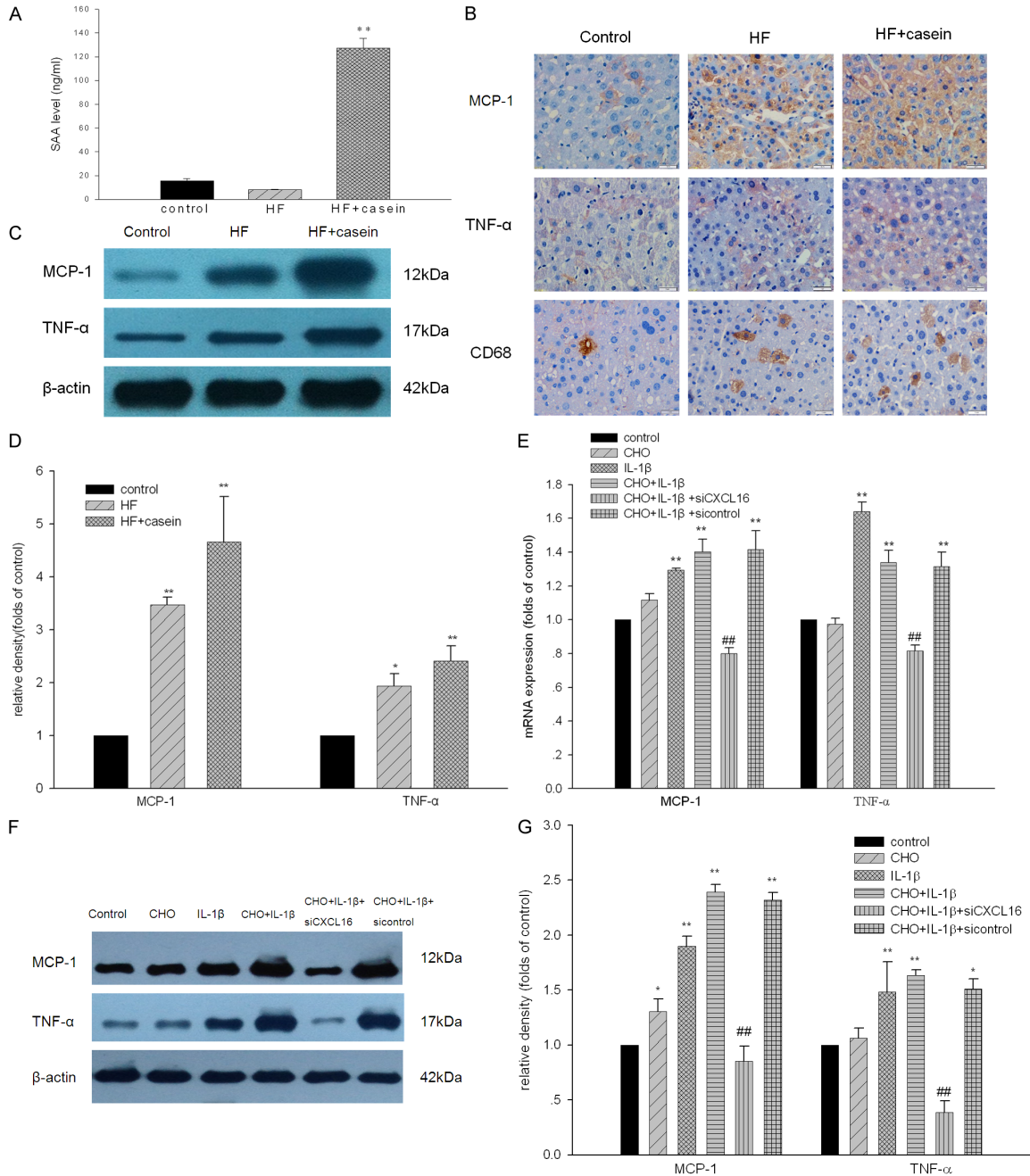
Figure 1. Establishment of inflamed NAFLD model. ApoE KO mice were fed with a normal diet containing 4% fat (Control), a high-fat diet containing 21% fat and 0.15% cholesterol (HF group), or a HF diet with 10% casein injection (HF+casein group) for 8 weeks (n=8). The levels of SAA in the serum of three groups were measured by enzyme linked immunosorbent assay (A). The results are expressed as the means ± SD (n=8). **$P<0.01$ *vs.* Control. The protein expression of CD68, TNF-α, and MCP-1 in the livers of the mice was measured by immunohistochemical staining (B, brown colour, original magnification ×400). The protein expression of TNF-α and MCP-1 in the livers of the mice was further checked by Western blotting. The identical total protein extracted from liver tissues was isolated by gel electrophoresis and transferred onto polyvinylidene difluoride membranes. The membranes were subjected to Western blotting using anti-mouse polyclonal antibodies against TNF-α, MCP-1, or β-actin which was used as an internal control. The histogram represents the means ± SD of the densitometric scans of the protein bands from the mice in each group, normalised by comparison with β-actin (C and D). *$P<0.05$ *vs.* Control, **$P<0.01$ *vs.* Control. HepG2 cells were treated without (Control) or with 30 μg/ml of cholesterol (CHO group), 5 ng/ml of IL-1β (IL-1β group), 30 μg/ml of cholesterol + 5 ng/ml of IL-1β (CHO+IL-1β group), 30 μg/ml of cholesterol + 5 ng/ml of IL-1β + CXCL16 siRNA (CHO+IL-1β + siCXCL16 group), or 30 μg/ml of cholesterol + 5 ng/ml of IL-1β + CXCL16 siRNA negative control (CHO+IL-1β + sicontrol group) for 24 hours. Total RNA was extracted from the HepG2 cells and cDNA

was aquired by reverse transcription. The mRNA expression of TNF-α and MCP-1 in HepG2 cells was determined by real-time PCR. β-actin served as the housekeeping gene (E). Results represent the means ± SD.**$P<0.01$ *vs.* Control, ##$P<0.01$ *vs.* CHO+IL-1β. The protein expression of TNF-α and MCP-1 in HepG2 cells was checked by Western blotting. The identical total protein extracted from the HepG2 cells was isolated by gel electrophoresis and transferred onto polyvinylidene difluoride membranes. The membranes were subjected to Western blotting using anti-human polyclonal antibodies against MCP-1, TNF-α, or anti-human monoclonal antibody against β-actin which was used as an internal control. The histogram represents the means ± SD of the densitometric scans for TNF-α and MCP-1, normalised by comparison with β-actin (F and G). *$P<0.05$ *vs.* Control, **$P<0.01$ *vs.* Control, ##$P<0.01$ *vs.* CHO+IL-1β.

Table 2. Biochemical data in the three groups of mice (means ± SD)

Indexes	Control group (n=8)	HF group (n=8)	HF+casein group (n=8)
TG (mmol/l)	3.1±0.6	7.5±2.0**	3.4±0.8##
TC (mmol/l)	13.7±2.7	27.8±4.0**	14.9±1.9##
HDL (mmol/l)	1.0±0.4	0.8±0.3	1.7±0.5*,##
LDL (mmol/l)	5.8±1.5	11.6±3.0**	9.5±1.3**,#

Compared to the controls, the mice fed with a high fat diet developed hyperlipidemia. The mice injected with 10% casein showed decreased plasma lipid concentrations compared with the HF group. TG: triglyceride, TC: total cholesterol, HDL: high-density lipoprotein, LDL: low density lipoprotein. *$P<0.05$ *vs.* Control, **$P<0.01$ *vs.* Control, #$P<0.05$ *vs.* HF group, ##$P<0.01$ *vs.* HF group.

protein expression of TNF-α, MCP-1, and CD68 in the livers of the HF+casein group compared with the HF group (**Figure 1B-D**). These findings suggest that systemic and local inflammation was successfully established in casein-injected mice. Furthermore, increased CD68 protein expression in the livers of casein-injected mice showed the infiltration of microphages subsequent to an inflammatory response. Results from *in vitro* studies further confirmed that IL-1β increased the mRNA and protein expression of TNF-α and MCP-1 in cholesterol-loaded HepG2 cells. Interestingly, the gene knockdown of CXCL16 expression by CXCL16 siRNA markedly decreased the expression of TNF-α and MCP-1 in IL-1β-treated HepG2 cells with cholesterol loading (**Figure 1E-G**).

Inflammation induced lipid accumulation in hepatic cells in vivo and in vitro

As shown in **Table 2**, plasma concentrations of TG, TC, and LDL in the HF group were significantly increased compared with the control. Although serum TG, TC, and LDL levels were decreased in the casein-injected ApoE KO mice compared with the HF group. HE staining and Filipin staining demonstrated that there was more significant lipid accumulation in the livers of casein-injected ApoE KO mice compared

with the HF group (**Figure 2A-C**). Results from *in vitro* studies further demonstrated that IL-1β stimulation contributed to lipid droplet accumulation in HepG2 cells (**Figure 2D** and **2E**). However, inhibition of CXCL16 expression by CXCL16 siRNA prevented lipid accumulation in HepG2 cells (**Figure 2DV**). Quantitative analysis of intracellular cholesterol further confirmed these results (**Figure 2C** and **2E**). These findings suggest that CXCL16 might be involved in the inflammation-mediated lipid accumulation in HepG2 cells.

Inflammation induced the activation of CXCL16/CXCR6 pathway in hepatic cells

Therefore we examined the effects of inflammation on the CXCL16/CXCR6 pathway in the presence or absence of lipid loading. As demonstrated by immunohistochemical staining, immunofluorescent staining, real-time PCR, and Western blotting, the results from *in vivo* and *in vitro* studies showed that inflammation exacerbated the increased mRNA and protein expression of CXCL16, CXCR6, and ADAM10 in hepatic cells induced by lipid loading compared with the control (**Figure 3A-F**). As expected, IL-1β up-regulated the expression of CXCL16, CXCR6, and ADAM10 in HepG2 cells (**Figure 3G**). However, these effects were inhibited by CXCL16 siRNA, suggesting that the CXCL16/CXCR6 pathway is activated by cholesterol loading and inflammation. In addition, we also noticed that the expression of ADAM10 constantly increased after cholesterol loading and IL-1β treatment, whereas CXCL16 siRNA could not prevent its expression.

Effects of CXCL16/CXCR6 pathway activation on the expression of ECM components and ROS production in hepatic cells

Collagen I and α-SMA are the main components of extracellular matrix (ECM) in livers. Therefore, we then examined the effects of inflammation on ECM expression in hepatic cells. We found
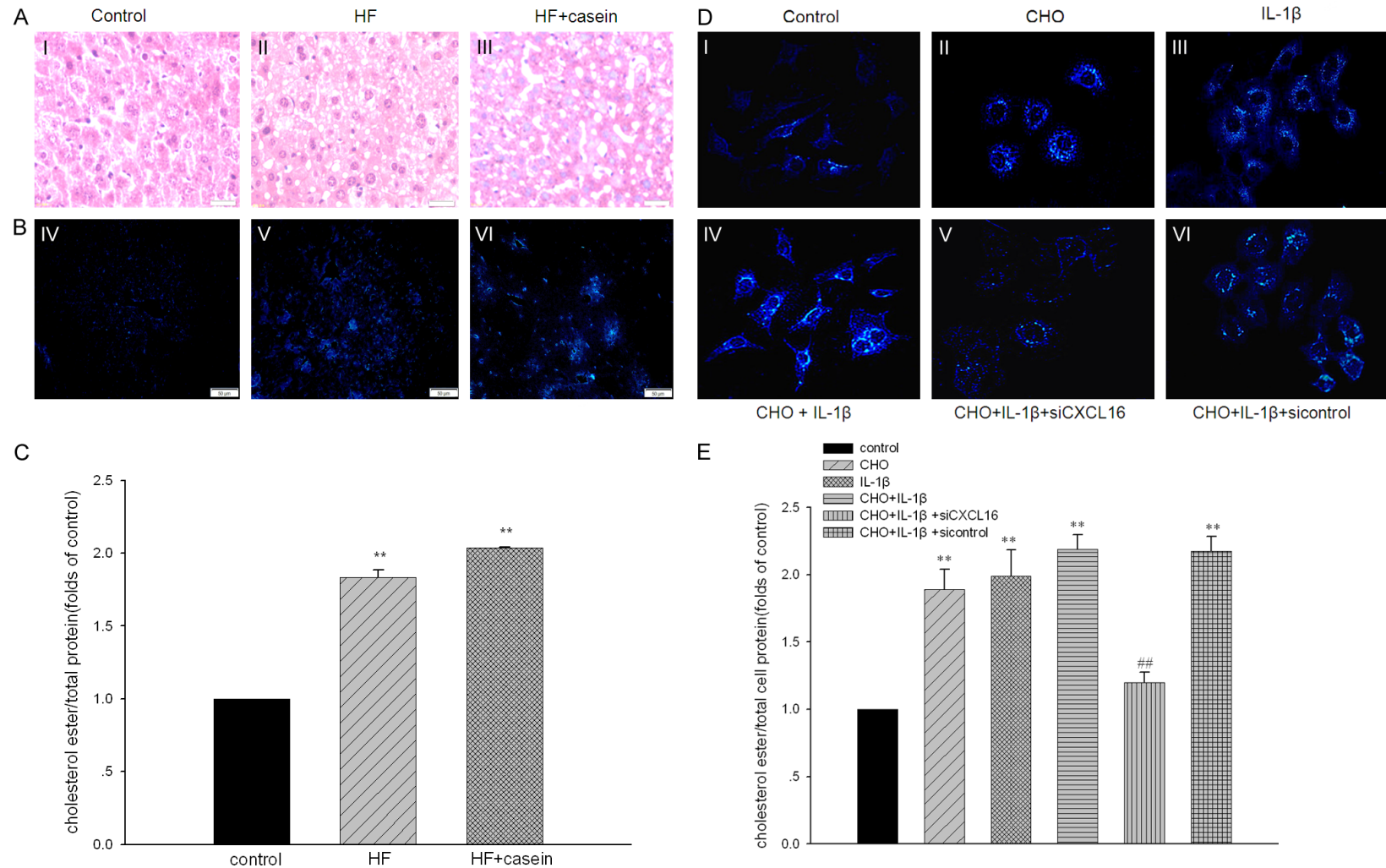
Figure 2. Inflammation induced lipid accumulation in hepatic cells *in vivo* and *in vitro*. ApoE KO mice were fed with a normal diet containing 4% fat (Control), a high fat diet containing 21% fat and 0.15% cholesterol (HF group), or with 10% casein injection (HF+casein group) for 8 weeks (n=8). The lipid accumulation in livers was checked by HE staining (A, I-III, ×400), Filipin staining (B, IV-VI, ×200). Quantitative assay of intracellular free cholesterol and cholesterol ester was used to further evaluate lipid accumulation in liver tissues (C). The results are expressed as the means ± SD (n=8). **$P<0.01$ *vs.* Control. HepG2 cells were treated without (Control) or with 30 µg/ml of cholesterol (CHO group), 5 ng/ml of IL-1β (IL-1β group), 30 µg/ml of cholesterol + 5 ng/ml of IL-1β (CHO+IL-1β group), 30 µg/ml of cholesterol + 5 ng/ml of IL-1β + CXCL16 siRNA (CHO+IL-1β + siCXCL16 group), or 30 µg/ml of cholesterol + 5 ng/ml of IL-1β + CXCL16 siRNA negative control (CHO+IL-1β + sicontrol group) for 24 hours. The lipid accumulation in HepG2 cells was checked by Filipin staining (D, I-VI, ×200). Quantitative assay of intracellular free cholesterol and cholesterol ester was used to check lipid accumulation as described in the section of materials and methods (E). Values are expressed as the means ± SD of triplicate wells from four experiments. **$P<0.01$ *vs.* Control, ##$P<0.01$ *vs.* CHO+IL-1β.
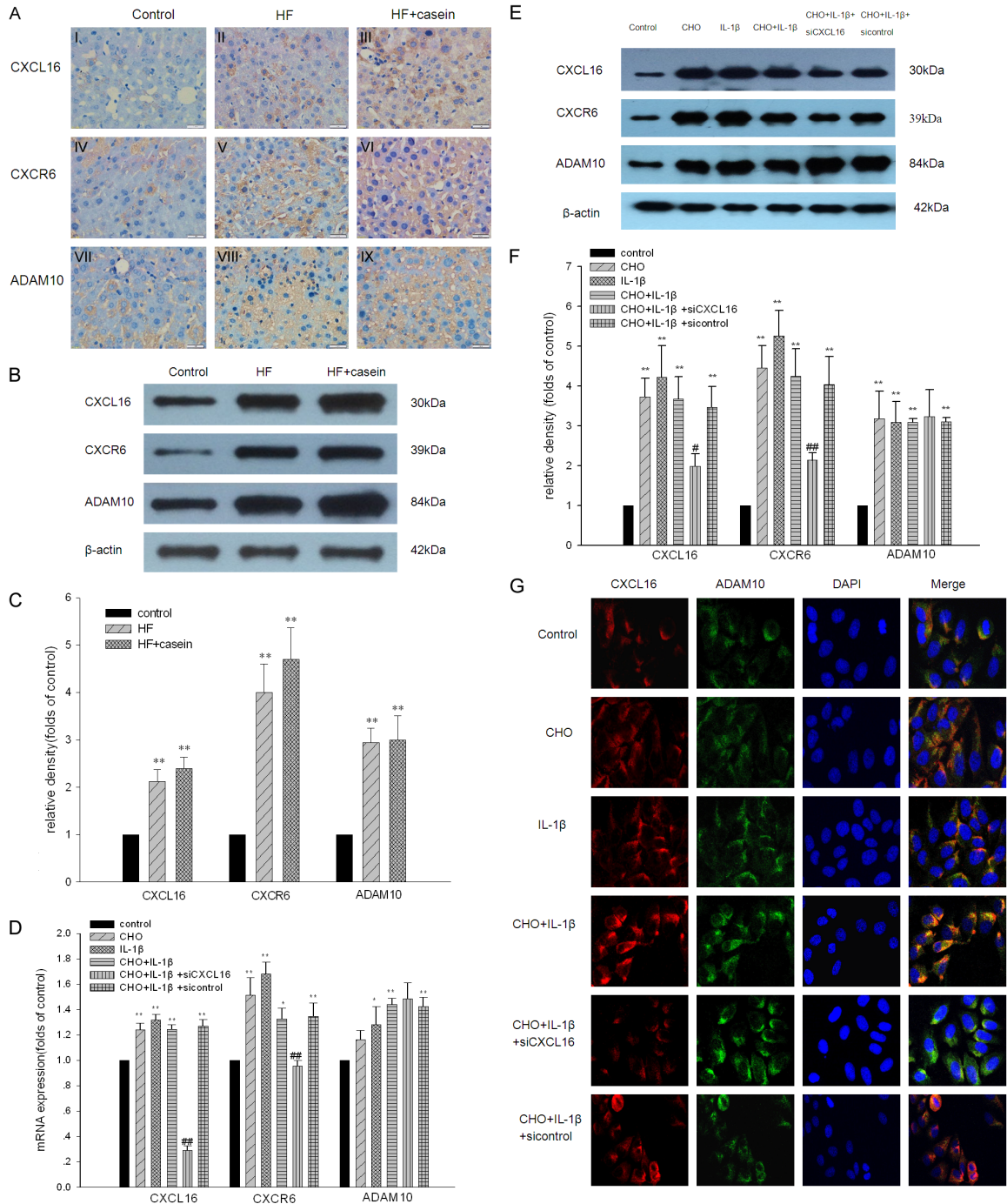
Figure 3. Inflammation induced the activation of the CXCL16/CXCR6 pathway in hepatic cells. ApoE KO mice were fed with a normal diet containing 4% fat (Control) a high fat diet containing 21% fat and 0.15% cholesterol (HF group), or a high fat diet with a 10% casein injection (HF+casein group) for 8 weeks (n=8). The protein expression of CXCL16/CXCR6 pathway components in the three groups of mice was checked by immunohistochemistry (A I-IX, ×400) and Western blotting. The identical total protein extracted from liver tissues was isolated by gel electrophoresis and transferred onto polyvinylidene difluoride membranes. The membranes were subjected to Western blotting using anti-mouse polyclonal antibodies against CXCL16, CXCR6, ADAM10, or β-actin which was used as an internal control. The histogram represents the means ± SD of the densitometric scans for the protein bands of CXCL16/CXCR6 pathway components, normalised by comparison with β-actin (B and C). **$P<0.01$ vs. Control. HepG2 cells were treated without (Control) or with 30 μg/ml of cholesterol (CHO group), 5 ng/ml of IL-1β (IL-1β group), 30 μg/ml of cholesterol + 5 ng/ml of IL-1β (CHO+IL-1β group), 30 μg/ml of cholesterol + 5 ng/ml of IL-1β + CXCL16 siRNA (CHO+IL-1β + siCXCL16 group), or 30 μg/ml of cholesterol + 5 ng/ml of IL-1β + CXCL16 siRNA negative control

(CHO+IL-1β + sicontrol group) for 24 hours. Total RNA was extracted from the HepG2 cells and cDNA was acquired by reverse transcription. The mRNA expression of CXCL16, CXCR6, and ADAM10 in HepG2 cells was determined by real-time PCR. β-actin served as the housekeeping gene (D). Results represent the means ± SD. *$P<0.05$ vs. Control, **$P<0.01$ vs. Control, #$P<0.05$ vs. CHO+IL-1β, ##$P<0.01$ vs. CHO+IL-1β. The protein expression of CXCL16, CXCR6, and ADAM10 in HepG2 cells was checked by Western blotting. The identical total protein extracted from the HepG2 cells was isolated by gel electrophoresis and transferred onto polyvinylidene difluoride membranes. The membranes were subjected to Western blotting using anti-human polyclonal antibodies against CXCL16, CXCR6, ADAM10, or anti-human monoclonal antibody against β-actin which was used as an internal control. The histogram represents means ± SD of the densitometric scans for CXCL16, CXCR6 and ADAM10, normalised by comparison with β-actin (E and F). *$P<0.05$ vs. Control, **$P<0.01$ vs. Control, #$P<0.05$ vs. CHO+IL-1β, ##$P<0.01$ vs. CHO+IL-1β. Immunofluorescent staining of CXCL16 and ADAM10 in HepG2 cells (G). The cells were stained with DAPI to visualise nuclei (blue), and with Alexa Fluor 488 and Alexa Fluor 594 to visualise the distribution of ADAM10 (green) and CXCL16 (red) proteins.
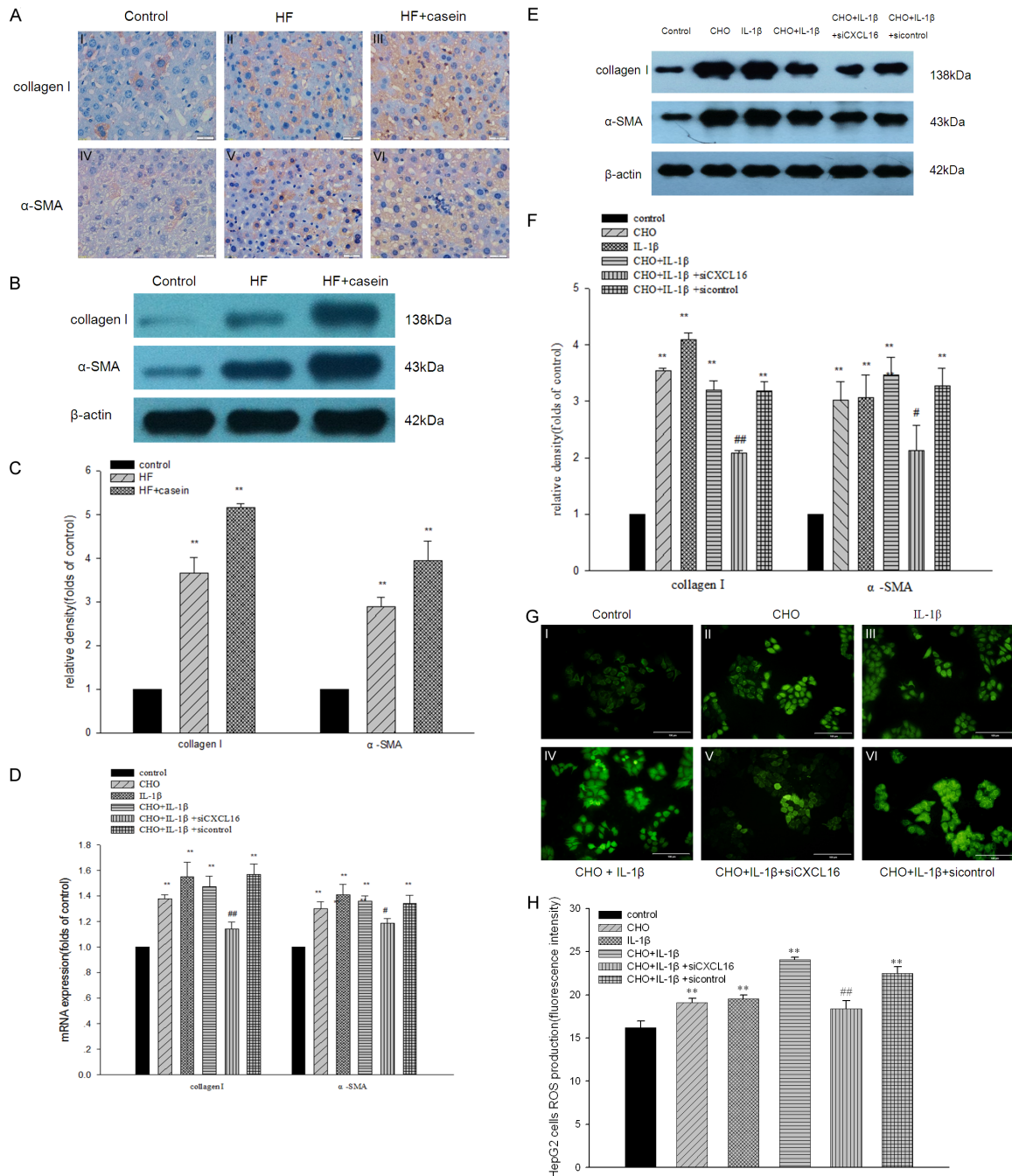
Figure 4. Effects of CXCL16/CXCR6 pathway activation on the expression of ECM components in the livers of ApoE KO mice and in HepG2 cells. ApoE KO mice were fed with a normal diet containing 4% fat (Control), a high fat diet containing 21% fat and 0.15% cholesterol (HF group), or with 10% casein injection (HF+casein group) for 8 weeks (n=8). Immunohistochemical staining shows the expression of collagen I and α-SMA in the livers of ApoE mice (A I-VI, ×400). The protein expression of collagen I and α-SMA in livers was checked by Western blotting. The identical total protein extracted from liver tissues was isolated by gel electrophoresis and transferred onto polyvinylidene difluoride membranes. The membranes were subjected to Western blotting using anti-mouse polyclonal antibodies against collagen I, α-SMA, or β-actin which was used as an internal control. The histogram represents the means ± SD of the densitometric scans for the protein bands of collagen I and α-SMA, normalised by comparison with β-actin (B and C). **$P<0.01$ *vs.* Control. HepG2 cells were treated without (Control) or with 30 μg/ml of cholesterol (CHO group), 5 ng/ml of IL-1β (IL-1β group), 30 μg/ml of cholesterol + 5 ng/ml of IL-1β (CHO+IL-1β group), 30 μg/ml of cholesterol + 5 ng/ml of IL-1β + CXCL16 siRNA (CHO+IL-1β + siCXCL16 group), or 30 μg/ml of cholesterol + 5 ng/ml of IL-1β + CXCL16 siRNA negative control (CHO+IL-1β + sicontrol group) for 24 hours. Total RNA was extracted from the HepG2 cells and cDNA was acquired by reverse transcription. The mRNA expression of collagen I and α-SMA was determined by real-time PCR. β-actin served as the housekeeping gene (D). Results represent the means ± SD. *$P<0.05$ *vs.* Control, **$P<0.01$ *vs.* Control, #$P<0.05$ *vs.* CHO+IL-1β, ##$P<0.01$ *vs.* CHO+IL-1β. The protein expression of collagen I and α-SMA in HepG2 cells was checked by Western blotting. The identical total protein extracted from the HepG2 cells was isolated by gel electrophoresis and transferred onto polyvinylidene difluoride membranes. The membranes were subjected to Western blotting using anti-human polyclonal antibodies against collagen I, α-SMA, or anti-human monoclonal antibody against β-actin which was used as an internal control. The histogram represents the means ± SD of the densitometric scans for the protein bands of collagen I and α-SMA, normalised by comparison with β-actin (E and F). **$P<0.01$ *vs.* Control, #$P<0.05$ *vs.* CHO+IL-1β, ##$P<0.01$ *vs.* CHO+IL-1β. HepG2 cells were washed with Dulbecco's phosphate buffered saline and incubated in the dark for 6 hours with 50 μmol/l 5-(and-6)-chloromethyl-2'7'-dichlorodihydrofluorescein diacetate (green fluorescence) (G). The fluorescence intensities of ROS production was quantified by Cell Quest software. Data represent the means ± SD (H). **$P<0.01$ *vs.* Control, ##$P<0.01$ *vs.* CHO+IL-1β.

that inflammation exacerbated the increase of collagen I and α-SMA protein expression in hepatic cells compared with the control, as confirmed by immunohistochemical staining (**Figure 4AI-VI**). Western blotting analysis further confirmed the results from the immunohistochemical staining (**Figure 4B** and **4C**). Results from the *in vitro* study showed that the mRNA and protein expression of collagen I and α-SMA were significantly increased in IL-1β-stimulated hepatic cells with or without cholesterol loading compared with the control. However, these effects were inhibited by CXCL16 siRNA (**Figure 4D-F**). These results suggest that inflammation-mediated ECM production occurs via the activation of the CXCL16/CXCR6 pathway.

To investigate the effects of inflammation on ROS production in HepG2 cells with or without cholesterol loading, we analysed the fluorescence intensity of ROS-sensitive 5-(and-6)-chloromethyl-2'7'-dichlorodihydrofluorescein diacetate after the treatment of cholesterol loading and IL-1β stimulation. As shown in **Figure 4G** and **4H**, IL-1β significantly increased ROS production in HepG2 cells mediated by cholesterol loading. However, ROS production was significantly prevented by CXCL16 siRNA, which suggests that CXCL16/CXCR6 pathway activation may play crucial roles in inflammation-mediated ROS production from HepG2 cells.

Discussion

According to the hypothesis of NAFLD, lipid accumulation caused by lipid disorder is the "first hit" and the subsequent inflammation is the "second hit", which promotes the development of NAFLD. CXCL16, as a scavenger receptor, adhesion molecule, and chemokine, has cross-talk with inflammation and lipid disorders. In this study, we mainly observed the role of the CXCL16/CXCR6 pathway in the progression of NAFLD. We successfully induced systemic inflammation by subcutaneously injecting the high-fat-fed ApoE KO mice with 10% casein, as shown by the significantly increased plasma SAA level compared with the HF group. In addition, immunohistochemical staining and Western blotting showed that the expression levels of CD68, MCP-1, and TNF-α were significantly increased in the livers of casein-injected high-fat-diet fed mice. It is well-known that CD68 is a specific biomarker of macrophages [20]. These findings suggested that systemic and local inflammation was established, which confirmed that an inflamed NAFLD model was successfully induced. Meanwhile, serum TC, TG, and LDL levels in the casein-injected mice were lower than those in the HF group. However, Filipin staining and intracellular cholesterol quantitative assays showed that lipid accumulation was significantly increased in the livers of

casein-injected high-fat-diet ApoE KO mice. These results demonstrated that inflammatory stress markedly exacerbated lipid accumulation and induced lipid redistribution from the circulation to the hepatic cells, which was confirmed by our previous studies [21].

It has been reported that CXCL16 is involved in the pathogenesis of inflammatory diseases, such as atherosclerosis [22], cardiomyopathy [23], and membranous nephropathy [15]. In our study, the mRNA and protein expression levels of CXCL16 and CXCR6 were significantly increased in response to lipid loading and inflammatory stress. However, CXCL16 inhibition by siRNA overrode these effects, accompanied by decreased lipid accumulation and reduced inflammatory cytokine production, suggesting that the CXCL16/CXCR6 pathway may be involved in the development of NAFLD. It is clear that as a transmembrane protein, CXCL16 can act as a scavenger receptor for oxLDL uptake [24]. The accumulation of oxLDL resulted in foam cell formation. A recent study [25] showed that internalised macrophages from CXCL16-/- mice had significantly less oxLDL uptake compared to wild-type macrophages. Additionally, the CXCL16 level was significantly increased with the severity of renal injury caused by hypercholesterolemia and oxLDL generation after unilateral ureteral obstruction [26]. Furthermore, blocking antibodies against CXCL16 significantly decreased oxLDL uptake and reduced the development of macrophage-derived foam cells. When CXCL16 is in soluble form, it can be released from the cell membrane by ADAM10 and can act as a chemokine that attracts neutrophils and lymphocytes. Gutwein et al. [15] demonstrated that pro-inflammatory cytokines, such as TNF-α and IFN-γ, can increase cellular as well as soluble CXCL16 in cultured human podocytes. Smith et al. [27] found that IL-1β can promote CXCL16 release in endothelial cells, suggesting that soluble CXCL16 could be linked to atherogenesis, not only as a marker of inflammation but also as a potential inflammatory mediator. Meanwhile, the pro-inflammatory factors, MCP-1 and TNF-α, also increased in high-fat mice and cholesterol-loaded HepG2 cells, which suggests that the transmembrane-bound form of CXCL16 acts as an adhesion molecule at the same time. Moreover, lipid accumulation in livers and HepG2 cells was accompanied by increased expression of CXCL16 under the conditions of cholesterol enrichment or inflammatory stress, while CXCL16 siRNA inhibited these effects. These findings are consistent with our previous studies that showed that inflammatory stress and dyslipidemia synergise to cause organ injuries [21, 28, 29]. Meanwhile, these results also suggest that although lipid loading and inflammation both increase the expression of CXCL16, different stimulating factors determine the predominant form of CXCL16 and which functions it mainly performs. As the unique receptor of CXCL16, CXCR6 mediates CXCL16 signals to promote the adhesive function and direct migration of different CXCR6-positive inflammatory cells, leading to T lymphocyte homing and macrophage accumulation as well as vascular smooth muscle cell proliferation [30, 31]. Therefore, the expression of CXCR6 is identical with CXCL16 in our study, which has also been previously shown in prostate cancer [32] and periodontal diseases [33].

ADAM10 is a major protease responsible for the conversion of CXCL16 from a membrane-bound scavenger receptor to a soluble chemokine [34]. In our study, IL-1β stimulation increased the expression of ADAM10 to release more soluble CXCL16, which is in accordance with the findings of other studies [12, 33]. Interestingly, we found that the protein expression of ADAM10 was significantly increased in the livers of the HF group and in cholesterol-loaded HepG2 cells. At first glance, these findings seem to be in conflict with previous publications. In human embryonic kidney (HEK) 293 cells, increasing the cellular cholesterol content reduced the activity of ADAM10, as determined by measuring the amount of cleaved soluble amyloid precursor protein [35]. In human umbilical vein endothelial cells, cholesterol depletion with an accompanying increase in the fluidity of the erythrocyte membrane markedly accelerated pro-vibrio cholera cytolysin cleavage by ADAM10 [36]. The studies mentioned above examined ADAM10 in terms of its cleavage activity. However, fewer papers have investigated the expression of ADAM10. Saarela et al. [37] found that atherogenic lipids up-regulated CXCL16 and down-regulated ADAM10 in primary human monocyte-derived macrophages, resulting in the preferential expression of CXCL16 as the transmembrane form, not the soluble form. Gutwein et al. [15] found

that in kidney biopsies of patients with membranous nephropathy, increased glomerular CXCL16 expression was accompanied by high level of oxLDL and decreased expression of ADAM10. Nevertheless, some results from other studies were consistent with ours. Cholesterol stimulation may also up-regulate the expression of ADAM10, although the cleavage of CXCL16 was not predominant. Schramme *et al.* [38] demonstrated that variable CXCL16 expression and increased ADAM10 expression were observed in biopsy tissues from kidney transplanted patients with the diagnosis of acute interstitial rejection. Matthews *et al.* [39] showed that in human THP-1 cells, cholesterol enrichment increased the shedding of interleukin-6 receptor (IL-6R) compared with the control. The discrepancies among different studies could reflect a cell-type specific effect, which may depend on the availability of the specific protease in that cell type [15]. Moreover, it has recently been shown that depending on the stimuli used, different metalloproteinases can regulate the release of CXCL16. In COS cells, phorbol 12-myristate 13-acetate induced the release of CXCL16, which was primarily mediated by ADAM17 [15]. In the glomeruli of patients with membranous nephropathy, increased ADAM17 expression was detectable, and the knockdown of ADAM10 by siRNAs increased not only cellular CXCL16 expression but also enhanced the release of CXCL16 from human podocytes [15], suggesting that ADAM17 plays an important role in the cleavage of CXCL16 in patients with membranous nephropathy. Our study found that the protein expression of ADAM10 was significantly increased, but the change in ADAM10 mRNA expression was not statistically significant when stimulated by cholesterol loading. Actually, ADAM-mediated shedding occurs constitutively and after activation with a broad variety of stimuli. The shedding process can be regulated at different levels by mechanisms including transcriptional control, posttranslational modifications, enzyme stability, and cellular localisation [40, 41]. According to our results, we propose that cholesterol loading may mainly regulate ADAM10-mediated shedding at the posttranslational level. Furthermore, CXCL16 siRNA has no effect on the expression of ADAM10. The underlying mechanism needs to be elucidated. Considering the liver tissue *in vivo* and HepG2 cells *in vitro*, we cannot exclude a tissue-specific effect on

the expression of ADAM10. In fact, ADAM10 is over-expressed in human HepG2 cells. The siRNA-mediated knockdown of ADAM10 significantly inhibited the growth, migration, and invasion of HepG2 cells [42]. Pruessmeyer *et al.* [43] found that either increasing ADAM10 or ADAM17 activity could limit neurodegeneration or suppressing their activity can block inflammation or tumour growth. It is clear that more questions need to be answered in future research efforts.

After the initial hepatic infiltration, the liver becomes extremely vulnerable to a series of hits that may follow, leading to hepatocyte injury and finally progressing from steatosis to NASH, and even fibrosis [44]. Xia *et al.* [45] demonstrated that in response to angiotensin II, CXCL16 recruits macrophages, T cells, and myeloid fibroblasts into the kidney, leading to renal fibrosis. Matsushita *et al.* [46] found that soluble CXCL16 promoted an epithelial-mesenchymal transition (EMT)-associated phenotype characterised by impaired E-cadherin production and the induction of vimentin *in vitro*. Our study found that CXCL16 inhibition down-regulated the expression of ECM components in the livers of ApoE KO mice and in HepG2 cells, showing that CXCL16 plays a pivotal role in the pathogenesis of liver injury and fibrosis through the regulation of macrophage and T cell infiltration and ECM accumulation. Gutwein *et al.* [16] demonstrated that inhibition of oxLDL uptake by CXCL16 blocking antibodies abrogated fibronectin and ROS production and restored α3 integrin expression in human podocytes. Our *in vivo* and *in vitro* studies demonstrated that inflammation exacerbated lipid disorder-mediated ROS production in hepatic cells. Surprisingly, blocking CXCL16 expression by CXCL16 siRNA resulted in reduced ROS production accordingly.

In summary, inflammation contributes to the progression of NAFLD through the activation of the CXCL16/CXCR6 pathway. The up-regulated expression of CXCL16, as a scavenger receptor, increases oxLDL uptake to induce lipid accumulation in hepatic cells, resulting in the disruption of cholesterol homeostasis, subsequent ECM synthesis, and oxidative stress production. Additionally, increased soluble CXCL-16 excretion, as an adhesion molecule and a chemokine, recruits T cell infiltration, induces

more inflammatory cytokine production, and finally accelerates the progression of NAFLD. Increased understanding of the mechanisms of the activation of CXCL16/CXCR6 pathway will encourage researchers to identify reliable strategies to prevent the progression of NAFLD. Thus, CXCL16/CXCR6 pathway could be a potential target of drug intervention in NAFLD, especially in patients accompanied with chronic inflammation. Under this condition, anti-inflammatory therapy might be also essential for NAFLD patients.

Acknowledgements

Disclosure of conflict of interest

None.

Address correspondence to: Dr. Kun Ling Ma, Institute of Nephrology, Zhong Da Hospital, School of Medicine, Southeast University, NO.87, Ding Jia Qiao Road, Nanjing 210009, Jiangsu Province, China. Tel: 0086 25 83262442; E-mail: klma05@163.com

References

[1] Clark JM. The epidemiology of nonalcoholic fatty liver disease in adults. J Clin Gastroenterol 2006; 40: S5-S10.

[2] Day CP. Natural history of NAFLD: remarkably benign in the absence of cirrhosis. Gastroenterology 2005; 129: 375-378.

[3] Vansaun MN, Mendonsa AM, Lee GD. Hepatocellular proliferation correlates with inflammatory cell and cytokine changes in a murine model of nonalchoholic fatty liver disease. PLoS One 2013; 8: e73054.

[4] Cohen JC, Horton JD, Hobbs HH. Human fatty liver disease: old questions and new insights. Science 2011; 332: 1519-1523.

[5] Xiao J, Guo R, Fung ML, Liong EC, Tipoe GL. Therapeutic approaches to non-alcoholic fatty liver disease: past achievements and future challenges. Hepatobiliary Pancreat Dis Int 2013; 12: 125-135.

[6] Zimmermann HW, Tacke F. Modification of chemokine pathways and immune cell infiltration as a novel therapeutic approach in liver inflammation and fibrosis. Inflamm Allergy Drug Targets 2011; 10: 509-536.

[7] Shashkin P, Simpson D, Mishin V, Chesnutt B, Ley K. Expression of CXCL16 in human T cells. Arterioscler Thromb Vasc Biol 2003; 23: 148-149.

[8] Matloubian M, David A, Engel S, Ryan JE, Cyster JG. A transmembrane CXC chemokine is a ligand for HIV-coreceptor Bonzo. Nat Immunol 2000; 1: 298-304.

[9] Wilbanks A, Zondlo SC, Murphy K, Mak S, Soler D, Langdon P, Andrew DP, Wu L, Briskin M. Expression cloning of the STRL33/BONZO/TYMSTRligand reveals elements of CC, CXC, and CX3C chemokines. J Immunol 2001; 166: 5145-5154.

[10] Shimaoka T, Kume N, Minami M, Hayashida K, Kataoka H, Kita T, Yonehara S. Molecular cloning of a novel scavenger receptor for oxidized low density lipoprotein, SR-PSOX, on macrophages. J Biol Chem 2000; 275: 40663-40666.

[11] Lv Y, Hou X, Ti Y, Bu P. Associations of CXCL16/CXCR6 with carotid atherosclerosis in patients with metabolic syndrome. Clin Nutr 2013; 32: 849-854.

[12] Abel S, Hundhausen C, Mentlein R, Schulte A, Berkhout TA, Broadway N, Hartmann D, Sedlacek R, Dietrich S, Muetze B, Schuster B, Kallen KJ, Saftig P, Rose-John S, Ludwig A. The transmembrane CXC-chemokine ligand 16 is induced by IFN-gamma and TNF-alpha and shed by the activity of the disintegrin-like metalloproteinase ADAM10. J Immunol 2004; 172: 6362-6372.

[13] Izquierdo MC, Martin-Cleary C, Fernandez-Fernandez B, Elewa U, Sanchez-Nino MD, Carrero JJ, Ortiz A. CXCL16 in kidney and cardiovascular injury. Cytokine Growth Factor Rev 2014; 25: 317-325.

[14] Heydtmann M, Lalor PF, Eksteen JA, Hubscher SG, Briskin M, Adams DH. CXC chemokine ligand 16 promotes integrin-mediated adhesion of liver-infiltrating lymphocytes to cholangiocytes and hepatocytes within the inflamed human liver. J Immunol 2005; 174: 1055-1062.

[15] Gutwein P, Abdel-Bakky MS, Schramme A, Doberstein K, Kampfer-Kolb N, Amann K, Hauser IA, Obermuller N, Bartel C, Abdel-Aziz AA, El Sayed el SM, Pfeilschifter J. CXCL16 is expressed in podocytes and acts as a scavenger receptor for oxidized low-density lipoprotein. Am J Pathol 2009; 174: 2061-2072.

[16] Gutwein P, Abdel-Bakky MS, Doberstein K, Schramme A, Beckmann J, Schaefer L, Amann K, Doller A, Kampfer-Kolb N, Abdel-Aziz AA, El Sayed el SM, Pfeilschifter J. CXCL16 and ox-LDL are induced in the onset of diabetic nephropathy. J Cell Mol Med 2009; 13: 3809-3825.

[17] Wehr A, Baeck C, Heymann F, Niemietz PM, Hammerich L, Martin C, Zimmermann HW, Pack O, Gassler N, Hittatiya K, Ludwig A, Luedde T, Trautwein C, Tacke F. Chemokine receptor CXCR6-dependent hepatic NK T cell accumulation promotes inflammation and liver fibrosis. J Immunol 2013; 190: 5226-5236.

[18] Liu J, Ma KL, Zhang Y, Wu Y, Hu ZB, Lv LL, Tang RN, Liu H, Ruan XZ, Liu BC. Activation of mTORC1 disrupted LDL receptor pathway: a potential new mechanism for the progression of non-alcoholic fatty liver disease. Int J Biochem Cell Biol 2015; 61C: 8-19.

[19] Gamble W, Vaughan M, Kruth HS, Avigan J. Procedure for determination of free and total cholesterol in micro- or nanogram amounts suitable for studies with cultured cells. J Lipid Res 1978; 19: 1068-1070.

[20] Ji RC. Macrophages are important mediators of either tumor- or inflammation-induced lymphangiogenesis. Cell Mol Life Sci 2012; 69: 897-914.

[21] Ma KL, Liu J, Wang CX, Ni J, Zhang Y, Wu Y, Lv LL, Ruan XZ, Liu BC. Activation of mTOR modulates SREBP-2 to induce foam cell formation through increased retinoblastoma protein phosphorylation. Cardiovasc Res 2013; 100: 450-60.

[22] Barlic J, Zhu W, Murphy PM. Atherogenic lipids induce high-density lipoprotein uptake and cholesterol efflux in human macrophages by up-regulating transmembrane chemokine CXCL16 without engaging CXCL16-dependent cell adhesion. J Immunol 2009; 182: 7928-7936.

[23] Borst O, Schaub M, Walker B, Sauter M, Muenzer P, Gramlich M, Mueller K, Geisler T, Lang F, Klingel K, Kandolf R, Bigalke B, Gawaz M, Zuern CS. CXCL16 is a novel diagnostic marker and predictor of mortality in inflammatory cardiomyopathy and heart failure. Int J Cardiol 2014; 176: 896-903.

[24] Shimaoka T, Nakayama T, Hieshima K, Kume N, Fukumoto N, Minami M, Hayashida K, Kita T, Yoshie O, Yonehara S. Chemokines generally exhibit scavenger receptor activity through their receptor-binding domain. J Biol Chem 2004; 279: 26807-26810.

[25] Aslanian AM, Charo IF. Targeted disruption of the scavenger receptor and chemokine CXCL16 accelerates atherosclerosis. Circulation 2006; 114: 583-590.

[26] Zhao L, Wu F, Jin L, Lu T, Yang L, Pan X, Shao C, Li X, Lin Z. Serum CXCL16 as a novel marker of renal injury in type 2 diabetes mellitus. PLoS One 2014; 9: e87786.

[27] Smith C, Halvorsen B, Otterdal K, Waehre T, Yndestad A, Fevang B, Sandberg WJ, Breland UM, Frøland SS, Øie E, Gullestad L, Damas JK, Aukrust P. High levels and inflammatory effects of soluble CXC ligand 16 (CXCL16) in coronary artery disease: down-regulatory effects of statins. Cardiovasc Res 2008; 79: 195-203.

[28] Ma KL, Ruan XZ, Powis SH, Chen Y, Moorhead JF, Varghese Z. Inflammatory stress exacerbates lipid accumulation in hepatic cells and fatty livers of apolipoprotein E knockout mice. Hepatology 2008; 48: 770-781.

[29] Ma KL, Liu J, Ni J, Zhang Y, Lv LL, Tang RN, Ni HF, Ruan XZ, Liu BC. Inflammatory stress exacerbates the progression of cardiac fibrosis in high-fat-fed apolipoprotein E knockout mice via endothelial-mesenchymal transition. Int J Med Sci 2013; 10: 420-426.

[30] Borst O, Abed M, Alesutan I, Towhid ST, Qadri SM, Foller M, Gawaz M, Lang F. Dynamic adhesion of eryptotic erythrocytes to endothelial cells via CXCL16/SR-PSOX. Am J Physiol Cell Physiol 2012; 302: C644-C651.

[31] Galkina E, Harry BL, Ludwig A, Liehn EA, Sanders JM, Bruce A, Weber C, Ley K. CXCR6 promotes atherosclerosis by supporting T-cell homing, interferon-gamma production, and macrophage accumulation in the aortic wall. Circulation 2007; 116: 1801-1811.

[32] Lu Y, Wang J, Xu Y, Koch AE, Cai Z, Chen X, Galson DL, Taichman RS, Zhang J. CXCL16 functions as a novel chemotactic factor for prostate cancer cells in vitro. Mol Cancer Res 2008; 6: 546-554.

[33] Hosokawa Y, Hosokawa I, Ozaki K, Nakae H, Matsuo T. CXC chemokine ligand 16 in periodontal diseases: expression in diseased tissues and production by cytokine-stimulated human gingival fibroblasts. Clin Exp Immunol 2007; 149: 146-154.

[34] Gough PJ, Garton KJ, Wille PT, Rychlewski M, Dempsey PJ, Raines EW. A disintegrin and metalloproteinase 10-mediated cleavage and shedding regulates the cell surface expression of CXC chemokine ligand 16. J Immunol 2004; 172: 3678-3685.

[35] Kojro E, Gimpl G, Lammich S, Marz W, Fahrenholz F. Low cholesterol stimulates the nonamyloidogenic pathway by its effect on the alpha-secretase ADAM 10. Proc Natl Acad Sci U S A 2001; 98: 5815-5820.

[36] Reiss K, Cornelsen I, Husmann M, Gimpl G, Bhakdi S. Unsaturated fatty acids drive disintegrin and metalloproteinase (ADAM)-dependent cell adhesion, proliferation, and migration by

modulating membrane fluidity. J Biol Chem 2011; 286: 26931-26942.

[37] Saarela J, Metso J, Schneider WJ, Jauhiainen M. Avian phospholipid transfer protein causes HDL conversion without affecting cholesterol efflux from macrophages. Biochim Biophys Acta 2009; 1791: 781-789.

[38] Schramme A, bdel-Bakky MS, Gutwein P, Obermuller N, Baer PC, Hauser IA, Ludwig A, Altevogt P, Gauer S, Hillmann A, Weide T, Jespersen C, Eberhardt W, Pfeilschifter J. Characterization of CXCL16 and ADAM10 in the normal and transplanted kidney. Kidney Int 2008; 74: 328-338.

[39] Matthews V, Schuster B, Schutze S, Bussmeyer I, Ludwig A, Hundhausen C, Sadowski T, Saftig P, Hartmann D, Kallen KJ, John SR. Cellular cholesterol depletion triggers shedding of the human interleukin-6 receptor by ADAM10 and ADAM17 (TACE). J Biol Chem 2003; 278: 38829-38839.

[40] Edwards DR, Handsley MM, Pennington CJ. The ADAM metalloproteinases. Mol Aspects Med 2008; 29: 258-289.

[41] Murphy G. Regulation of the proteolytic disintegrin metalloproteinases, the 'Sheddases'. Semin Cell Dev Biol 2009; 20: 138-145.

[42] Yuan S, Lei S, Wu S. ADAM10 is overexpressed in human hepatocellular carcinoma and contributes to the proliferation, invasion and migration of HepG2 cells. Oncol Rep 2013; 30: 1715-1722.

[43] Pruessmeyer J, Ludwig A. The good, the bad and the ugly substrates for ADAM10 and ADAM17 in brain pathology, inflammation and cancer. Semin Cell Dev Biol 2009; 20: 164-174.

[44] Yilmaz Y. Review article: is non-alcoholic fatty liver disease a spectrum, or are steatosis and non-alcoholic steatohepatitis distinct conditions? Aliment Pharmacol Ther 2012; 36: 815-823.

[45] Xia Y, Entman ML, Wang Y. Critical role of CXCL16 in hypertensive kidney injury and fibrosis. Hypertension 2013; 62: 1129-1137.

[46] Matsushita K, Toiyama Y, Tanaka K, Saigusa S, Hiro J, Uchida K, Inoue Y, Kusunoki M. Soluble CXCL16 in preoperative serum is a novel prognostic marker and predicts recurrence of liver metastases in colorectal cancer patients. Ann Surg Oncol 2012; 19: S518-S527.